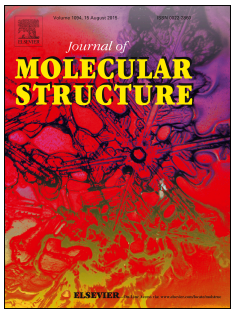

A Pd(II) complex derived from pyridine-2-carbaldehyde oxime ligand: Synthesis, characterization, DNA and BSA interaction studies and *in vitro* anticancer activity

Moloud Alinaghi, Kazem Karami, Azar Shahpiri, Akram Kazemi nasab, Amir Abbas Momtazi-borojeni, Elham Abdollahi, Janusz Lipkowski

PII: S0022-2860(20)30804-8

DOI: https://doi.org/10.1016/j.molstruc.2020.128479

Reference: MOLSTR 128479

To appear in: *Journal of Molecular Structure*

Received Date: 3 March 2020

Revised Date: 14 May 2020

Accepted Date: 16 May 2020

Please cite this article as: M. Alinaghi, K. Karami, A. Shahpiri, A.K. nasab, A.A. Momtazi-borojeni, E. Abdollahi, J. Lipkowski, A Pd(II) complex derived from pyridine-2-carbaldehyde oxime ligand: Synthesis, characterization, DNA and BSA interaction studies and *in vitro* anticancer activity, *Journal of Molecular Structure* (2020), doi: https://doi.org/10.1016/j.molstruc.2020.128479.

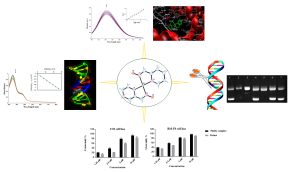

A Pd(II) complex derived from pyridine-2-carbaldehyde oxime ligand: synthesis, characterization, DNA and BSA interaction studies and *in vitro* anticancer activity

Moloud Alinaghi[a], Kazem Karami*[a], Azar Shahpiri [b], Akram Kazemi nasab[b], Amir Abbas Momtazi-borojeni[c,d], Elham Abdollahi[d], Janusz Lipkowski[e].

[a]*Department of Chemistry, Isfahan University of Technology, Isfahan, 84156/83111, Iran*
[b]*Department of Agricultural Biotechnology, Isfahan University of Technology, Isfahan 84156-83111, Iran*
[c]*Nanotechnology Research Center, Bu-Ali Research Institute, Mashhad University of Medical Sciences, Mashhad, Iran*
[d]*Department of Medical Biotechnology, School of Medicine, Student Research Committee, Mashhad University of Medical Sciences, Mashhad, Iran*
[e]*Institute of Physical Chemistry, Polish Academy of Sciences, Kasprzaka 44/52, 01-224 Warsaw, Poland*

Abstract

A novel Pd(II) complex, $[Pd(C_6H_5N_2O)_2]$, containing pyridine-2-carbaldehyde oxime ligand has been synthesized and characterized using elemental analysis, Fourier-transform infrared, nuclear magnetic resonance and mass spectroscopy. The single crystal structure of this Pd(II) complex has been determined by X-ray crystallography. Based on the DNA binding studies including ultraviolet visible spectrophotometry, fluorescence emission titration and viscosity measurement, the interaction of Pd(II) complex with calf thymus DNA occurs by groove binding. In the absence of an external reductant, the Pd(II) complex cleaves the supercoiled double-stranded DNA under physiological conditions. Moreover, in the presence of Pd(II) complex, the Bovine Serum Albumin microenvironment and secondary structure change. On the basis of the competitive experiments using site markers, the complex is mainly located in site I of the protein. The binding of the Pd(II) complex to DNA was modeled using molecular docking. The antitumor impacts of the ligand and the Pd(II) complex were evaluated *in vitro* against the mouse colon carcinoma (C26) and melanoma (B16-F0) tumor cell lines. The antitumor activity has been significantly improved by the complexation process. IC_{50} values smaller than those of cisplatin have been shown by the Pd(II) complex and oxime ligand against cancer cell lines. In addition, Pd(II) complex has been tested against NIH normal fibroblast cells. Consequently, Pd(II) complex may be considered a selective compound against cancer cells, according to the SI definition.

Keywords:
Palladium(II) complex; Pyridine-2-carbaldehyde oxime; DNA interactions; BSA interaction; Molecular docking; *In vitro* cytotoxicity

1. Introduction

Metal complexes, which can cleave DNA under physiological conditions, have recently been of interest both for their possible applications in artificial nucleic acid chemistry and the development of anticancer agents based on metals [1-3].

The side effects of cisplatin limit its potential efficiency despite its activity in the treatment of several cancers types [4, 5]. The mechanism of cisplatin action includes binding to DNA in a covalent manner [6]. Thus, the development of more efficient, target specific, less hazardous and cytotoxic drugs, which bind non-covalently to DNA, is inevitable.

The most abundant proteins in the circulatory system, serum albumins, are well known for acting as transporters of several compounds [7], such as drugs and nutrients, mainly by forming non-covalent complexes as specific binding sites. Thus, the absorption, distribution, metabolism, excretion properties, stability and toxicity of chemical substances can be remarkably affected by their binding activities to serum albumins [8]. Bovine Serum Albumin has been extensively investigated because of its homologous structure to Human Serum Albumin [9].

Considering the unique capability of biologically active organic ligands to bind with different biological targets, their coordination to transition metal ions is reportedly promising [10]. Oximes are a group of important functional ligands applied in medicine [11-13], magnetism [14], catalysis [15] and crystal engineering [16-18]. Oximes are universal ligands easily designed to form compounds of different properties. In general, there is one active nitrogen in the neutral oxime group, >C=NOH, which binds to metal cations. Thus, it functions as a terminal-coordinated monodentate ligand. However, a large number of possibilities are created to affect the coordination mode by using different substituents in the oxime carbon depending on the additional coordination sites in the substituents such as those in pyridine [19-22]. Moreover, the position of the coordinative atoms in the substituent strongly affects the structure of the material, as observed in the coordination of 2-pyridyl oxime, which usually generates a chelating mononuclear complex, compared with 3-pyridyl or 4-pyridyl oxime, which preferably yields polymeric chain like structures *via* terminal coordination [23]. In addition, complexes with a large variety of nuclearity can be formed by the deprotonation of the oxime OH group using the negatively charged oxygens for additional coordination [17, 18, 24]. A lot of hydrolytic processes including acyl, phosphoryl or sulfuryl transfer or cleavage *via* attacking an electrophilic center, are responsible for the strong nucleophilicity of

the oximate anion (>C=N−O$^-$) [25]. The distinct capability of a family of pyridyl oximes for reactivation of acetylcholinesterase enzyme (AChE) upon complete inhibition by organophosphorus compounds as pesticides and chemical warfare agents is particularly interesting from the pharmaceutical aspect [26-30]. In addition, a wide range of biological applications of pyridyl oxime derivatives such as sedative, anti-depressant, anti-spasmodic, analgesic and anti-inflammatory among others in cardiovascular system has been studied [31]. The studies on the coordination chemistry of pyridine-2-carbaldehyde oxime were first carried out in the late fifties and early sixties. Single crystal X-ray structures were not available back then. According to the physical and spectroscopic data based studies, intramolecular hydrogen bonding in the type of structure can be formed by the square planar cationic complexes of divalent transition metals [32-34]. $[Cu_3(OH)(SO_4)\text{-}\{(py)CHNO\}_3]$ was the first structurally characterized pyridine-2-carbaldehyde oxime metal complex [35]. The 2,6-diacetylpyridine dioxime (dapdoH_2) monoanion was originally considered a tridentate chelate in palladium(II) and platinum(II) chemistry. [PdCl(dapdoH)] and [PtCl(dapdoH)] have been biologically evaluated [36].

In this work, a novel Pd(II) complex, $[Pd(C_6H_5N_2O)_2]$, containing pyridine-2-carbaldehyde oxime ligand has been prepared. Elemental analysis, Fourier-transform infrared, nuclear magnetic resonance and mass spectroscopy have been used to characterize the complex. The single crystal structure of this Pd(II) complex was determined by X-ray crystallography. Electronic absorption titration, fluorescence spectroscopy and viscosimetric measurement were used to study the DNA and BSA binding behaviors of this compound. Furthermore, the DNA cleavage activity of the Pd(II) complex and oxime ligand has been measured. In addition, molecular docking studies have been used to obtain detailed information on the binding of the complex with DNA and BSA. Finally, the cytotoxic activity of compounds against mouse colon carcinoma (C26), mouse melanoma (B16-F0) and normal fibroblast cells (NIH) has been evaluated using MTT assay.

2. Experimental Section

2.1. Materials

Commercial grade reagents in this work were used as received. Reagent grade Calf-thymus DNA (CT-DNA), BSA and methylene blue (MB) were supplied by Sigma Aldrich Chemical Co. Extra pure solvents applied in the syntheses and physical measurements and analytical reagent grade. Tris(hydroxymethyl)-aminomethane (Tris-HCl) buffer were provided by

Merck Chemical Co. Stock solutions of oxime ligand and other solutions were prepared using doubly distilled deionized water. Stock solutions of concentrated Pd(II) complex were prepared in DMSO solvent and the appropriate dilutions were prepared using Tris-HCl buffer at pH 7.2 to obtain the concentrations required throughout the experiments. Maximum concentration of DMSO was 0.1% v/v. Stock solutions of CT-DNA and BSA were prepared by dissolution in 5 mM Tris buffer and 50 mM NaCl at pH 7.2. Reagents and cell culture media were purchased from Gibco Company (Germany).

2.2. Methods and Instrumentation

An FT-IR JASCO 680-PLUS spectrophotometer was used to record FT-IR spectra in the 400-4000 cm^{-1} region using potassium bromide pellets. A JASCO 7580 UV-Vis-NIR double beam spectrophotometer was used to record the electronic absorption spectra in a 1 cm path length cell. Fluorescence spectra were recorded in solution using a Cary Eclipse fluorescence spectrophotometer. NMR spectra were recorded at 400.13 MHz (^{1}H) and 100.61 MHz $^{13}C\{^{1}H\}$ using a Bruker spectrometer. A Leco CHNS-932 apparatus was used to perform elemental analyses. An Agillent 6410 QQQ spectrophotometer was used to record mass spectra. A Cannon Fenske routine viscometer was used to perform viscometric titrations at a constant temperature of 298.0 (±0.1) K in thermostatic water bath.

2.3. Syntheses

2.3.1. Synthesis of pyridine-2-carbaldehyde oxime ligand ($C_6H_5N_2O$)

0.276 g of hydroxylamine hydrochloride (4 mmol) was slowly added to 190.2 µL of 2-pyridinecarboxaldehyde (2 mmol) in ethanol, followed by the dropwise addition of an aqueous 2 mM solution of sodium hydroxide. The clear solution thus formed was stirred at 50 °C for 2 h. Removal of the solvent by evaporation yielded the ligand as a white precipitate.

(Yield: 93.4%). IR (KBr, cm^{-1}) ν ($C\text{-}H_{Ph}$) = 3186-3004, ν ($C\text{-}H_{imine}$) = 2882-2775, ν ($C{=}N_{imine}$) = 1657.ν ($C{=}N_{pyridine}$) = 1619. ^{1}H NMR (DMSO-d_6, ppm): δ= 7.38 (ddd, 1H, H_b), 7.78-7.84 (m, 2H, H_c, H_d), 8.07 (s, 1H, HC=N), 8.57 (br d, 1H, H_a), 11.74 (br s, 1H, OH).

2.3.2. Synthesis of Pd(II) complex [$Pd(C_6H_5N_2O)_2$]

0.04 g of the oxime ligand (0.3 mmol) and 0.024 g of sodium acetate (0.3 mmol) were dissolved in a solvent mixture containing acetonitrile (10 ml) and water (1 ml), and the mixture obtained was stirred at ambient temperature for about 20 min. A solution of 0.08 g of $Pd(OAc)_2$ (0.36 mmol) in 5 ml of acetonitrile was added in a dropwise manner to the system, which was then refluxed at 60 °C for 6 h to obtain a dark green solution. The mixture

was concentrated to 2 ml, followed by adding 15 ml of n-hexane to precipitate a dark green powder, which was then dried at room temperature.

(Yield: 76.9%). Anal. Calc. for $C_{12}H_{10}N_4O_2Pd$ (%) C, 41.38; H, 2.87; N, 16.09. Found C, 41.27; H, 2.63; N, 16.23. IR (KBr, cm^{-1}) ν (C-H_{Ph}) = 3049-3008, ν (C-H_{imine}) =2955, 2852, ν (C=N_{imine}) = 1612, ν (C=$N_{pyridine}$) = 1608. ^{1}H NMR (DMSO-*d_6*, ppm): δ= 7.4 (dd, 1H, H_b), 7.54 (d, 1H, H_d), 7.74 (s, 1H, HC=N), 8.02 (dd, 1H, H_c), 9.65 (d, 1H, H_a). ^{13}C{^{1}H} NMR (DMSO-*d_6*, ppm): 118.6 (C_b), 120.04 (C_d), 140.02 (C=N), 140.5 (C_c), 146.5 (C_e), 157.4 (C_a). ESI-MS, m/z (%): 348.8 [M + H].

2.4. Crystallography

X-ray diffraction experiments were performed using an Agilent SuperNova single crystal diffractometer (Cu K(a) radiation at 150 K. The analytical numeric absorption corrections were made using a multi-faceted crystal model based on expressions derived by R.C. Clark & J.S. Reid was used to make [37]. SHELXS97 and SHELXL (Sheldrick 2008) programs were used to solve and refine the structures by direct methods.

2.5. DNA Binding Experiments

CT-DNA experiments, were carried out in Tris-HCl buffer solution (pH=7.2). CT-DNA solutions showed a UV absorbance ratio (A_{260}/A_{280}) of > 1.8, indicating the DNA purity [38]. Absorption spectroscopy by the molar absorption coefficient (ε = 6600 M^{-1} cm^{-1}) at 260 nm was use to find the DNA concentration per nucleotide [39, 40]. Absorption spectral titration experiments were performed at constant 60 µM concentration of the Pd(II) complex, changing CT-DNA concentration in the range of 0.0-120 µM. In addition, viscosity measurements were used to further study the Pd(II) complex binding mode. The mean values of three replicate measurements were used in the evaluation of sample viscosities. Relative specific viscosity $(\eta/\eta_0)^{1/3}$ values, in which η and η_0 are the specific viscosity contributions of DNA in the presence (η) and absence (η_0) of each compound, respectively, were plotted *vs*. r (r = [complex]/[DNA]) [41]. The relation η = (t - t_0)/t_0, in which t_0 and t indicate the flow times of the blank buffer and DNA containing solutions, respectively, was used to calculate the relative viscosities [42]. The competitive experiment was performed to study the ability of the Pd(II) complex to remove methylene blue from DNA methylene blue mixture. The DNA-methylene blue solution ([DNA]/[methylene blue] = 5) was excited at a wavelength of 630 nm in the absence and presence of various complex concentrations [43].

2.6. DNA Cleavage Experiments

DNA cleavage was examined using agarose gel electrophoresis carried out by incubation at 37 °C as follows: plasmid PUC57 (0.01 M) in 5 mM Tris buffer (pH=7.2) was subjected to treatment with oxime ligand or Pd(II) complex, followed by incubation for 3 h. The samples were then examined by electrophoresis for 1 h at 135 V on 0.07% agarose gel using tris-boric acid-EDTA buffer. Following electrophoresis, the bands were visualized using UV light and photographed. The cleavage mechanism of PUC57 was studied in the presence of H_2O_2, DMSO and NaN_3 as the oxidizing agent, hydroxyl scavenger and singlet oxygen scavenger, respectively.

2.7. Protein Binding Studies

The stock solution of Bovine Serum Albumin was prepared by dissolving the proper amount of BSA in the buffer solution, which contained 5 mM Tris-HCl/50 mM NaCl at pH 7.2, and stored at 4 °C for further application. UV visible absorption spectroscopy was used to obtain BSA concentration using ε_{280} = 44300 $M^{-1}cm^{-1}$ [44]. Absorption titration experiments were performed by keeping BSA concentration constant at 6 µM while different concentrations of the complex were added (0.0-12 µM). During the absorption spectral measurements, identical amounts of Pd(II) complex solution were added to both the BSA and the reference solutions in order to exclude the absorbance due to the complex. In the tryptophan fluorescence quenching experiment, the tryptophan residues of BSA [45] were quenched by maintaining the BSA concentration constant at 6 µM while changing the concentration of the complex (quencher) in the range of 0.0-12 µM to provide solutions with different molar ratios of quencher to BSA. Having added the quencher, the fluorescence spectra were recorded at excitation and emission wavelengths of 280 and 343 nm, respectively, in the fluorometer. Site competitive replacement tests were performed in the presence of Warfarin, Ibuprofen and Digoxin site markers by fluorescence titration method to find the binding location of Pd(II) complex on BSA. Equal concentrations of BSA and site marker (6 µM) were used, followed by slow addition of Pd(II) complex. The fluorescence spectra were recorded at 298 K with an excitation wavelength and emission of 280 nm and 300-500 nm, respectively.

2.8. Molecular Docking

Auto Dock 4.2 package was used to carry out molecular docking studies by the Lamarckian genetic algorithm (LGA) [46, 47]. Conversion of CIF file using Mercury software gave the PDB format of Pd(II) complex. The initial Bovine Serum Albumin structure was taken from the Protein Data Bank (PDB ID: 4F5S) at a resolution of 2.47 Å. DNA sequence was also

obtained from the Protein Data Bank (PDB ID: 3U2N) at a resolution of 1.25 Å. Chain (A) of BSA and all the other hetero atoms including water molecules were separated during preparation input files. The suitable binding site for complex-DNA interaction and BSA was found by blind docking [48, 49]. Afterwards, focus docking was carried out on the best location. Biomolecule structures were limited to a grid box with 60 × 60 × 60 $Å^3$ dimensions and a 0.375 Å grid spacing, which involved nearly all the macromolecules. All other parameters were maintained at their default values.

2.9. Culture Medium and Cell Lines

The National Cell Bank of Pasteur Institute, Tehran, Iran, provided melanoma B16F0 and colon carcinoma C26 cancer cell lines. Cells were cultured in Dulbecco's Modified Eagle Medium (DMEM), which was supplemented with 10% heat inactivated fetal bovine serum (FBS), 100 $U.ml^{-1}$ penicillin, 100 $\mu g.ml^{-1}$ streptomycin and 5 mM L-glutamine. Afterwards, the cell lines were grown at the temperature of 37 °C in a humidified atmosphere which contained 5% CO_2.

2.10. MTT Assay

MTT [3-(4,5-dimethylthiazol-2-yl)-2,5-diphenyl-tetrazolium bromide] colorimetric assay was employed to study the cytotoxicity of the complex and ligand. 200 µl of cells (5×10^4 $cells.ml^{-1}$) were seeded in 96 well microplates, followed by incubation in 37°C and 5% CO_2 for 24 h to perform the cytotoxicity assay. Afterwards 20 µl of the solutions at specific concentrations (in DMSO) of the oxime ligand and Pd(II) complex were added to the wells. The control and treated solutions included the same DMSO concentration [0.5% (v/v)]. 20 µl of MTT solution (5 $mg.ml^{-1}$ in phosphate buffer solution) were added 48 h through the incubation, followed by incubation for another 3 h. Subsequently, the formazan crystals formed were dissolved by slow replacement of 150 µl of the medium containing MTT with DMSO. An ELISA plate reader was then used to determine the absorbance at 560 nm. Each test was performed in triplicate. Non-linear regression of concentration-response curves of the complex against each tested cell line was used to calculate IC_{50} (concentration inhibiting the cell growth by 50%) values.

3. Results and discussion

3.1. Synthesis of the complex and characterization by spectroscopic methods

$[Pd(C_6H_5N_2O)_2]$ was prepared by reacting oxime ligand with palladium acetate (1:1.2 molar ratio) in acetonitrile and water at 60 °C (Scheme 1).

The characteristic bands at 1657 and 1619 cm^{-1} in the IR spectrum of oxime ligand are associated with (C=N) stretching vibrations of oxime and pyridine groups. ν (C=N) has been shifted to a lower frequency in the Pd(II) complex, which shows the nitrogen atom of imine group has bonded to the metal cation [50].

In the ^{1}H NMR spectrum of the oxime, the aromatic protons (H_a, H_b, H_c and H_d) appear at 7.4-8.5 ppm. Since these protons are non-equivalent, splitting and formation of doublets are observed (Fig S1). As observed in Scheme 2, H_b has been split by other hydrogens and appears as a doublet of doublets at 7.38 ppm. H_c and H_d signals have merged and appear at 7.78-7.84 ppm. H_a has resonated as a broad doublet at 8.57 ppm. These protons show up at different frequencies (7.4-9.65 ppm) in the ^{1}H NMR spectrum of Pd(II) complex (Fig S2). In the complex spectrum, H_a and H_d appear as doublets. Furthermore, H_b and H_c are represented by a doublet of doublets, which indicates the disappearance of $^{4}J_{H-H}$. Furthermore, a singlet can be observed at 8.07 ppm in the oxime spectrum, which is associated with the imine protons of the ligand that has been shifted to a lower frequency (7.74 ppm) because of generation of the complex. As Fig. S1 shows, a broad singlet is observed in the ^{1}H NMR spectrum of the ligand at 11.74 ppm. This singlet, which is not observed in the Pd(II) complex spectrum, corresponds to O-H proton of the oxime ligand. Six types of carbon are present in the ^{13}C NMR spectrum of the complex (Fig. S3) in the 118.6-157.4 ppm range.

Positive ion Electrospray Ionization Mass Spectrum of the complex shows a major peak at m/z = 348.8, which is attributed to the $[M + H]^{+}$ (Fig. S4).

3.2. Molecular Structure of Pd(II) Complex

Single crystal X-ray diffraction in the solid phase has been used to characterize the Pd(II) complex The slow diffusion of hexane into a CH_2Cl_2 solution yielded suitable crystals. Fig. 1 shows the ORTEP diagram of the Pd(II) complex.

Table 1 shows the corresponding crystallographic data and structural refinement details and the selected bond lengths and angles are summarized in Table 2. This complex was crystallized in the triclinic space group *P1* with Z=2. In this complex, the coordination number around the palladium atom is four, which indicates that Pd(II) atom is bonded to two oxime ligands from two imino nitrogens and two pyridine nitrogen atoms of the ligands. The sum of angles around palladium atom is 360.3° for Pd1, the distortion being the most

pronounced in the relatively decreasing "bite" angle of the metalated moiety. The bond angles of N1-Pd1-N2 and N3-Pd1-N4 are forced to 80.2(4) and 79.7(3)°, respectively, by the restraints of the five membered ring. Palladium(II) metal square planar geometry is slightly tetrahedrally distorted and the mean deviations from the least square plane are only 0.030 Å. The Pd-N bond lengths are 2.031(9) and 2.041 (9) Å for Pd1-N1 and Pd1-N3, respectively, and 2.035(8) Å for Pd1-N2 and Pd1-N4, which are longer than the sum of the covalent radii of Pd and N(sp^2) atoms (2.011 Å) [51]. In addition, N-O bond lengths in this complex fall in the ranges found for the corresponding complexes [20, 52].

3.3. DNA Binding Experiments

3.3.1. Electronic Absorption Titration

Molar absorptivity considerably decreases when CT-DNA is added to Pd(II) complex in 5 mM Tris-HCl/50 mM NaCl buffer at pH 7.2 (Fig. 2). The binding of the complex to DNA *via* groove binding mode is suggested by the hypochromic change observed without any shift in its electronic spectrum [53, 54]. The intrinsic binding constants, K_b, of the Pd(II) complex is obtained by the analysis of the absorption spectral data using Eq. 1 to enable the quantitative comparison of the DNA binding affinities [55].

$$[\mathrm{DNA}]/(\varepsilon_a - \varepsilon_f) = [\mathrm{DNA}]/(\varepsilon_b - \varepsilon_f) + 1/(\mathrm{K}_b\,(\varepsilon_b - \varepsilon_f)) \qquad (1)$$

in which [DNA] and ε_a, which is found by calculation of A_{obs}/[complex], are the concentration of DNA in base pairs and the apparent extinction coefficient, respectively, and ε_f and ε_b are the extinction coefficients of the Pd(II) complex in its free form and the complex in the bound form, respectively. Fitting the set of data into the above equation gives a straight line with a slope and y-intercept of $1/(\varepsilon_b - \varepsilon_f)$ and $1/K_b(\varepsilon_b - \varepsilon_f)$, respectively. The slope to intercept ratio gives K_b (Fig. 2, inset). The value of the obtained intrinsic binding constants, K_b, ($1.44\times10^5\ M^{-1}$) is lower than those observed for proven intercalators (EtBr and methylene blue with K_b values of 3.3×10^5 and $3.45\times10^5\ M^{-1}$, respectively) [56, 57].

Equation 2 was used to calculate the free energy (ΔG) of compound-DNA complex by using the values of binding constant (K_b):

$$\Delta G = -RT \ln K_b \qquad (2)$$

Binding constant shows the stability of the compound-DNA complex while free energy is a measure of the spontaneity/non-spontaneity of the compound-DNA binding. A negative free energy was found for the Pd(II) complex (-7.04 kcal mol^{-1}), which indicates that compound-DNA interaction is spontaneous.

3.3.2. Emission Experiments of Competitive DNA Binding

A comparative binding study was carried out using methylene blue to figure out if the Pd(II) complex binding with DNA is of the groove or the intercalative type. Methylene blue (MB), which is a phenothiazinium dye, reportedly bonds with nucleic acids. The binding of methylene blue to DNA is presumably stabilized by the planar heterocyclic dye *via* favorable stacking interactions with its neighboring base pairs [58]. The intercalative binding of MB with DNA can be used to rationalize the great quenching in the MB emission intensity in the DNA environment [59], which is expected given the intercalation mechanism [59, 60]. The DNA bound MB emission spectra have been monitored in the presence of different complex concentrations (Fig. S5). Based on the experimental results, the complex addition to the DNA bound methylene blue did not lead to the release of methylene blue molecules whereas the fluorescence intensity continuously reduced, implying that the two probes, complex and methylene blue, independently bond with DNA and the binding of one probe was not influenced by that of the other. The interaction of Pd(II) complex with the DNA was a groove interaction, as verified experimentally [54, 61].

3.3.3. Viscosity Measurements

DNA viscosity is sensitive to the variations in DNA length. The relationship between the relative viscosity (η/η_0) and DNA length (L/L_0) is shown by $L/L_0 = (\eta/\eta_0)^{1/3}$, where L and L_0 are the apparent molecular lengths in the presence and absence of the compound, respectively [62]. The relative specific viscosities of methylene blue and Pd(II) complex $(\eta/\eta_0)^{1/3}$, were plotted *vs*. r (r = [compound]/[DNA]) (fig. S6). As the amount of methylene blue increases, the DNA relative viscosity is continuously enhanced, which is in agreement with the lengthening of the DNA helix. The viscosity of DNA solutions significantly increases by the intercalation because of DNA helix lengthening when the base pairs are separated to incorporate the aromatic chromophore of the bound molecule. It is attractive to associate the increased viscosity observed with the intercalative interaction of methylene blue [63]. Interestingly, the specific viscosity of DNA slightly decreases for the Pd(II) complex. Little or no change is observed in the DNA solution viscosity when small molecules

exclusively bind in the DNA grooves under identical conditions [42, 64]. These results again suggest the interaction of Pd(II) complex with the groove of DNA, as verified by the above findings.

3.3.4. DNA Cleavage Studies

Metallonucleases have the potential for application in cancer therapy [65]. Some of the clinically approved anticancer agents aim at the cell death by cleaving DNA [66, 67]. The DNA cleavage ability of transition metal complexes is an effective means to study the mechanism of toxicity and artificial nuclease abilities. The DNA-cleavage reactions consist of three steps: formation of supercoiled, open circular and linear forms (Forms I, II and III, respectively). The intact supercoil form (Form I) will rather quickly migrate upon exposure of circular plasmid DNA to electrophoresis. If scission takes place on one strand (nicking), the supercoil will relax to form a slower moving open circular form (form II). The cleavage of both strands gives rise to a linear form (form III) migrating between Forms I and II [68].

DNA cleavage without added reductant: The nuclease activity of pyridine-2-carbaldehyde oxime ligand and its Pd(II) complex in physiological conditions was investigated utilizing pUC57 plasmid DNA in 5 mM Tris buffer (pH = 7.2) medium without external agents. Different Pd(II) complex concentrations can cleave a pUC57 plasmid DNA (Form I) into a nicked form (Form II) (Fig. 3, lines 2–8). No cleavage was observed in the DNA cleavage experiments carried out with oxime ligand (Fig. 3, lines 9–11). In addition, this shows the concentration dependence of DNA cleavage activity of the Pd(II) complex.

DNA cleavage with added reductant: Considerable nuclease activity on supercoiled DNA was shown by the Pd(II) complex in the absence of external agents in a concentration dependent manner. Pd(II) complex cleaved supercoiled form (Form I) only produced nicked circular form (Form II) and no linear form (Form III) in the absence of H_2O_2 (an oxidizing agent) (Fig. 3, lines 2-8). The activity of DNA cleavage in the absence of an oxidant is often hydrolytic rather than oxidative [3]. Nevertheless, the most impressive characteristic is that a higher nuclease activity of the complex and linear form (Form III) is observed in the presence of H_2O_2 (Fig. 4, line 3). Pd(II) complex DNA cleavage can be efficiently promoted in the presence of hydrogen peroxide, according to the results [69]. In addition, oxime ligand exhibited no significant nuclease in the absence of H_2O_2 (Fig. 3, lines 9-11). However, in the presence of H_2O_2, impressive cleavage of circular plasmid DNA, which converts Form I to Form II, is shown by the ligand (Fig. 4, line 5), indicating an oxidative cleavage process [70].

The test was performed in the presence of DMSO and NaN_3 as the hydroxyl radical scavenger and singlet oxygen quencher, respectively, to determine the DNA cleavage mechanism by Pd(II) complex and oxime ligand. The efficiency of DNA cleavage by the complex was not significantly reduced in the presence of DMSO (Fig. 4, line 2). However, the cleavage activity of the Pd(II) complex was significantly inhibited by the addition of NaN_3 singlet quencher (Fig. 4, line 4). Singlet oxygen causes the DNA cleavage, based on the results [71]. The experimental results also show that NaN_3 and DMSO significantly inhibit the cleavage activity of the oxime ligand (Fig. 4, lines 6 and 7), indicating the important parts of hydroxyl radical and singlet oxygen in the DNA cleavage in the presence of H_2O_2.Oxime ligand cleaves DNA by oxidative cleavage, according to the results [72].

3.4. BSA Binding Experiments

3.4.1. Absorption Spectral Studies

In order to study the nature of the quenching process, UV-Visible absorption titration of BSA with the Pd(II) complex was carried out. The quenching mechanism may be of dynamic or static type. Dynamic quenching takes place in the case of an interaction between a quencher and the fluorophore in a short lived excited state whereas static quenching occurs upon the complex formation between the fluorophore and a quencher in the ground state [73]. In the UV spectrum of BSA, two absorption bands are observed; a strong band corresponding to the protein backbone and a weak band associated with aromatic amino acids at 200 and 278 nm, respectively (Fig. 5) [74]. Absorption intensity decreases on the addition of the Pd(II) complex to BSA without influencing the absorption band position. This verifies that the interaction of Pd(II) complex with BSA changes the microenvironment of the three aromatic amino acid residues [1]. In addition, this indicates that a complex-BSA system formation in the ground state leads to a static interaction between the complex and BSA [75].

3.4.2. Fluorescence Spectroscopic Studies

The interaction between the Pd(II) complex with BSA by tryptophan emission quenching experiments has been examined in this study. BSA itself shows emission at 345 nm due to the presence of tryptophan residue in its amino acid sequence [76]. The fluorescence intensity progressively decreases on the addition of successive amounts of the Pd(II) complex to BSA (Fig. 6). Eq. 3 is used after correction for the inner-filter effect [77]

$$I_{corr} = I_{obs}\, e^{(A_{ex}+A_{em})/2} \qquad (3)$$

I_{corr} and I_{obs} are the corrected and measured fluorescence, respectively, and A_{em} and A_{ex} are the absorbance of the complex at the emission and excitation wavelengths, respectively. The corrected fluorescence quenching data were analyzed using the Stern-Volmer equation [78]

$$\frac{I_0}{I} = 1 + K_{SV}[Q] = 1 + K_q\tau_0[Q] \qquad (4)$$

I and I_0 are the fluorescence intensities in the presence and absence of the complex, respectively, $K_{sv,}$ [Q], k_q and τ_0 are the Stern-Volmer quenching constant, quencher concentration, bimolecular quenching rate constant and average lifetime of the fluorophore without quencher, respectively. The slope of the plot of I_0/I *vs*. [Q] can be used to obtain K_{SV} (Fig. 6 insets). The calculated K_{sv} value for Pd(II) complex is $3.51 \times 10^4 M^{-1}$. The τ_0 value for tryptophan fluorescence in proteins is 2×10^{-8} s [79], the following equation can be used to calculate the quenching rate constant (k_q):

$$k_q = K_{SV}/\tau_0 \qquad (5)$$

The quenching constant (k_q) obtained for Pd(II) complex was 1.75×10^{12} $M^{-1}s^{-1}$. This is greater than the value anticipated for a purely dynamic quenching mechanism ($2.0 \times 10^{10} M^{-1}s^{-1}$). This verifies that a static quenching mechanism has happened [80]. The quenching interaction and the number of binding sites (n) can be calculated using the following equation assuming similar, independent binding sites in the biomolecule for the static binding constant (K_b) [81]÷

$$\text{Log}\frac{(I_0 - I)}{I} = \text{Log}\, K_b + n\, \text{Log}\,[Q] \qquad (6)$$

where n and K_b are the number of binding sites and binding constant, respectively. $\text{Log}[(I_0 - I)/I]$ *vs*. log[Q] plots are linear (Fig. S7). K_b can be used to calculate the intercept and slope of such plots. An n value near unity indicates a single binding site type for the complex on BSA (Table 3). The binding free energy of Pd(II) complex to BSA is −6.23 kcal mol^{-1}.

3.4.3. Site Selective Binding

The free and bound forms of the complex can also be affected by the competition of drugs for binding sites on serum albumin. Thus, the identification of the complex binding site in BSA is important. The crystal structure of Bovine Serum Albumin indicates that it consists of three similar domains, referred to as I, II, and III, each one including A and B sub-domains [82]. Site marker competitive tests using markers specifically binding to a specific site on BSA, are

carried out to find the binding site of the complex on BSA. When two or more drugs are used in any biological system, each one tries to tie itself to binding sites faster than the other. The drug with a closer resemblance to the protein can replace the other one. In this work, the specificity of the drug binding was recognized by carrying out competition experiments using Warfarin, Ibuprofen and Digoxin. In these titrations, the BSA to probe concentration ratio was 1:1 (6×10^{-6} M: 6×10^{-6} M) (Fig. S8). When the site markers were added into the BSA solution, the fluorescence intensity remarkably decreased. Plots of $\log[(I_0 - I)/I]$ *vs.* log[complex] were obtained for comparison of the effect of Warfarin, Ibuprofen and Digoxin on the binding of the complex to BSA (Table 3). The complex-BSA binding constant is 3.71 $\times 10^4 M^{-1}$, which is decreased in the presence of Warfarin. This indicates the competition between Warfarin and the complex. Therefore, Pd(II) complex binds to site I of serum albumin. Docking studies further verify this observation, as will be subsequently discussed.

3.4.4. The Fluorescence Resonance Energy Transfer (FRET) from BSA to the Pd(II) Complex

Bovine Serum Albumin emission is quenched in the presence of the Pd(II) complex, according to the fluorescence spectral changes. This indicates the major overlap of the tryptophan (Trp) emission spectrum in BSA and the Pd(II) complex absorption spectrum, resulting in the transfer of energy from the excited state BSA to the Pd(II) complex [83]. In general, radiative and non-radiative energy transfers are possible. Förster's resonance energy transfer (FRET) theory, which is applied in the determination of the distance between the acceptor (*i.e.* drug's binding site) and the donor (*i.e.* tryptophan residue of BSA), clarifies non-radiative energy transfer [84]. Eq. 7 may be applied to find the energy transfer efficiency between the acceptor (A) and the donor (D), E, based on the FRET theory [85]:

$$E = 1 - \left(\frac{I}{I_0}\right) = \frac{1}{1+(r/R_0)^6} \qquad (7)$$

where I and I_0 are the BSA fluorescence intensities measured in the presence and absence of the Pd(II) complex, r is the distance between A and D and R_0, which is obtained suing Eq. 8, is the critical distance when the energy transfer efficiency is 50% [86]:

$$R_0^6 = 8.79 \times 10^{-25} K^2 N^{-4} \Phi J \qquad (8)$$

where K^2, N, Φ and J are the dipole orientation factor, medium (solution) refractive index, fluorescence quantum yield of D in the absence of A, and overlap integral of the absorption spectrum of A with the fluorescence emission spectrum of D, respectively (Fig. 7).

Eq. 9 is used to obtain the J value [86]:

$$J = \frac{\int f_D(\lambda)\varepsilon_A(\lambda)\lambda^4 d\lambda}{\int f_D(\lambda)d\lambda} \quad (9)$$

where $f_D(\lambda)$ and $\varepsilon_A(\lambda)$ are the fluorescence intensity of D and the molar absorption coefficient of A at wavelength λ, respectively. The J value was found to be 8.262×10^{-14} cm^3 L mol^{-1} for the Pd(II) complex. The E, R_0, and r values found for the binding of the Pd(II) complex to BSA, obtained using $K^2 = 2/3$, N = 1.336, and Φ = 0.15, were 0.25, 3.63 nm, and 4.36 nm, respectively. The D-to-A distances (r) calculated were below 8 nm and the r values were bigger than the corresponding value for R_0 ($0.5R_0 < r < 1.5R_0$). The energy transfer from BSA to complex takes place with a great chance and the quenching mechanism is static for the interaction, according to the results [87].

3.5. Molecular Docking

3.5.1. Docking with DNA

Pd(II) complex binds to the minor groove of DNA, AT-rich sequence, as shown by the molecular docking analysis (Fig. 8). A hydrogen bond is formed between the Pd(II) complex (oxime ligand oxygen) and the adenine base of DNA. The relative binding energy of the docked structure for the Pd(II) complex with the DNA molecule (ΔG_b) was calculated to be -7.7 kcal mol^{-1}. This indicates the reasonable comparability of the results of the absorption titration tests (-7.04 kcal mol^{-1}) with those found using the computational method.

3.5.2. Docking with BSA

The Pd(II) complex is situated in domain I, as Fig. 9 shows. A hydrogen bond between the Pd(II) complex oxygen atom and Glu 125 (2.2 Å) is observed. The amino acid residues of BSA, which interacted with the complex, are Phe 36, Pro 113, Lys 114, Leu 115, Lys 116, Leu 122, Glu 125, Phe 133, Lys 136, Tyr 139 and Tyr 160. Furthermore, the distance between the Pd(II) complex and Trp 134 residue is 7.0 Å. The best ΔG_b value for the interaction of BSA with the complex determined was found to be -7.44 kcal mol^{-1} which is in conformity with the binding free energy found using the experimental value of K_b (-6.23 kcal mol^{-1}).

3.6. *In vitro* Selective-Cytotoxic Activity

Melanoma B16F0 and colon carcinoma C26 cell lines were treated with Pd(II) complex and oxime ligand at the concentration range of 1.25-10 µM to assess the *in vitro* cytotoxicity of the compounds against cancer cells. The cytotoxicity of the compounds after 48 h was measured using MTT-assay method, which is a well-documented bioassay. The cytotoxic

activity of Cis-platin, a standard anti-cancer drug, was investigated for the sake of comparison under identical experimental conditions. Concentration dependent cytotoxicity against both cancer cell lines is shown by the compounds (Fig. S9). The high and low Pd(II) complex and oxime ligand concentrations (10 and 1.25 μM, respectively) against C26 cancer cells showed (93.56 and 84.32%) and (21.09 and 14.28%) cytotoxicity, respectively. The corresponding cytotoxicity values in the case of B16F0 cancer cell line were (97.36% and 91.56%) and (39.98% and 33.8%), respectively. While important and high cytotoxic activity was shown by the compounds against both B16F0 and C26 cancer cell lines, low toxicity was identified against NIH normal cells in comparison with cisplatin (Table 4). Therefore, Pd(II) complex shows higher cytotoxicity against both cancer cell lines compared with oxime ligand. Remarkably low cytotoxic activity was shown by both compounds against normal cells with IC_{50} values of >100 μM. Thus, the cytotoxicity of the compounds against normal cells was lower compared with cisplatin. The results are in compliance with the other experimental data, which indicate the inhibitory effect of palladium complexes on cancer cells. Palladium complexes were found to have significant cytotoxicity against various cancer cells such as MCF-7 breast cancer cell line [88]. According to other *in vitro* studies, saccharinate and/or terpyridine complexes of palladium inhibit the concentration dependent growth of MCF-7 and MDA-MB-231 breast cancer cell lines at IC_{50} values of up to 3.05 and 0.09 μM, respectively [89, 90]. *In vivo* study on Walker tumor bearing rats further verify these results. Therefore, natural biocompounds derived palladium complexes inhibit tumor growth by 90%. [91]. The SI values, found by comparing the IC_{50} of the complexes against each cancer cell with that of the normal cell line to assess the selective effect of the compounds against cancer cells, are some of the other significant results of this *in vitro* cytotoxicity study [92]. The SI values of both compounds exceeded 2. Consequently, both compounds have potential selective cytotoxicity on cancer cells. The results are further confirmed by the previous reports on more cytotoxic activity to cancer cells compared with the normal cells [93-99] arising from the cancer cell sensitivity to the death complexes. To summarize, important selective concentration dependent cytotoxic activity on proliferation and viability of breast and colon cancer cells, *in vitro*, has been shown by both compounds. However, it is necessary to confirm anticancer effects using validated *in vivo* studies.

4. Conclusion

A novel Pd(II) complex bearing pyridine-2-carbaldehyde oxime ligand has been prepared in the present work. X-ray crystallographic study of the Pd(II) complex indicates a square planar

coordination around the Pd(II) ion with a little tetrahedrally distorted. The DNA binding properties of the complex were investigated using electronic absorption, fluorescence spectroscopy and viscosity measurements. The interaction of the Pd(II) complex with DNA is of groove binding type, based on the results. In addition, the Pd(II) complex could cleave the supercoiled plasmid under physiological conditions without any additional reductants. The reactivity towards BSA showed a static emission quenching by the complex. The binding distances of Pd(II) complex with BSA were calculated to be 4.36 nm, based on the Foster's theory. According to the competitive studies using Warfarin, Ibuprofen and Digoxin site markers, and the complex was mainly located in site I of the protein. The binding of the Pd(II) complex to DNA and BSA was modeled by molecular docking. The cytotoxic investigations indicate that the Pd(II) complex has high cytotoxic activity against various cell lines tested. Moreover, the cytotoxicity results indicated the higher efficiency of Pd(II) complex compared with the corresponding free ligand under the same experimental conditions.

Acknowledgments

The authors gratefully acknowledge the financial support of this research by the Isfahan University of Technology (IUT).

References:

[1] X.-F. Zhao, Y. Ouyang, Y.-Z. Liu, Q.-J. Su, H. Tian, C.-Z. Xie, J.-Y. Xu, Two polypyridyl copper (II) complexes: synthesis, crystal structure and interaction with DNA and serum protein in vitro, New J. Chem., 38 (2014) 955-965.
[2] M. Ganeshpandian, R. Loganathan, S. Ramakrishnan, A. Riyasdeen, M.A. Akbarsha, M. Palaniandavar, Interaction of mixed ligand copper (II) complexes with CT DNA and BSA: Effect of primary ligand hydrophobicity on DNA and protein binding and cleavage and anticancer activities, Polyhedron, 52 (2013) 924-938.
[3] F. Darabi, H. Hadadzadeh, J. Simpson, A. Shahpiri, A water-soluble Pd (II) complex with a terpyridine ligand: experimental and molecular modeling studies of the interaction with DNA and BSA; and in vitro cytotoxicity investigations against five human cancer cell lines, New J. Chem., 40 (2016) 9081-9097.
[4] E. Wong, C.M. Giandomenico, Current status of platinum-based antitumor drugs, Chem. Rev., 99 (1999) 2451-2466.
[5] B. Rosenberg, L. Vancamp, J.E. TROSKO, V.H. MANSOUR, Platinum compounds: a new class of potent antitumour agents, Nature, 222 (1969) 385-386.
[6] E.R. Jamieson, S.J. Lippard, Structure, recognition, and processing of cisplatin− DNA adducts, Chem. Rev., 99 (1999) 2467-2498.
[7] B.X. Huang, H.-Y. Kim, C. Dass, Probing three-dimensional structure of bovine serum albumin by chemical cross-linking and mass spectrometry, J. Am. Soc. Mass Spectrom., 15 (2004) 1237-1247.
[8] N. Shahabadi, M. Maghsudi, Z. Kiani, M. Pourfoulad, Multispectroscopic studies on the interaction of 2-tert-butylhydroquinone (TBHQ), a food additive, with bovine serum albumin, Food chem., 124 (2011) 1063-1068.

[9] Y.-J. Hu, Y. Liu, X.-S. Shen, X.-Y. Fang, S.-S. Qu, Studies on the interaction between 1-hexylcarbamoyl-5-fluorouracil and bovine serum albumin, J. Mol. Struct., 738 (2005) 143-147.
[10] G. Gasser, I. Ott, N. Metzler-Nolte, Organometallic anticancer compounds, J. Med. Chem., 54 (2010) 3-25.
[11] C. Biswas, M. Zhu, L. Lu, S. Kaity, M. Das, A. Samanta, J.P. Naskar, A palladium (II) complex: Synthesis, structure, characterization, electrochemical behavior, thermal aspects, BVS calculation and antimicrobial activity, Polyhedron, 56 (2013) 211-220.
[12] R. Sun, Y. Li, M. Lü, L. Xiong, Q. Wang, Synthesis, larvicidal activity, and SAR studies of new benzoylphenylureas containing oxime ether and oxime ester group, Bioorg. Med. Chem. Lett., 20 (2010) 4693-4699.
[13] M. Kurtoğlu, S.A. Baydemır, Studies on mononuclear transition metal chelates derived from a novel (E, E)-dioxime: synthesis, characterization and biological activity, J. Coord. Chem., 60 (2007) 655-665.
[14] D.P. Giannopoulos, A. Thuijs, W. Wernsdorfer, M. Pilkington, G. Christou, T.C. Stamatatos, Supramolecular chains of high nuclearity {Mn III 25} barrel-like single molecule magnets, Chem. Commun., 50 (2014) 779-781.
[15] T. Kluge, M. Bette, T. Rüffer, C. Bruhn, C. Wagner, D. Ströhl, J.r. Schmidt, D. Steinborn, Activation of Acetyl Ligands through Hydrogen Bonds: A New Way to Platinum (II) Complexes Bearing Protonated Iminoacetyl Ligands, Organometallics, 32 (2013) 7090-7106.
[16] S. Pramanik, S. Roy, T. Ghorui, S. Ganguly, K. Pramanik, Molecular and electronic structure of nonradical homoleptic pyridyl-azo-oxime complexes of cobalt (III) and the azo-oxime anion radical congener: an experimental and theoretical investigation, Dalton Trans., 43 (2014) 5317-5334.
[17] K.F. Konidaris, M. Kaplanis, C.P. Raptopoulou, S.P. Perlepes, E. Manessi-Zoupa, E. Katsoulakou, Dinuclear versus trinuclear complex formation in zinc (II) benzoate/pyridyl oxime chemistry depending on the position of the oxime group, Polyhedron, 28 (2009) 3243-3250.
[18] K. Karami, Z.M. Lighvan, S.A. Barzani, A.Y. Faal, M. Poshteh-Shirani, T. Khayamian, V. Eigner, M. Dušek, Design and synthesis of a novel trinuclear palladium (ii) complex containing an oxime chelate ligand: determining the interaction mechanism with the DNA groove and BSA site I by spectroscopic and molecular dynamics simulation approaches, New J. Chem., 39 (2015) 8708-8719.
[19] M. Nandy, S. Banerjee, C. Rizzoli, E. Zangrando, A. Nonat, L.J. Charbonnière, S. Mitra, Syntheses, structural diversity and photo-physical properties of copper (I) and silver (I) coordination polymers based on the pyridine-4-amidoxime ligand, Polyhedron, 65 (2013) 252-261.
[20] C. Papatriantafyllopoulou, C.G. Efthymiou, C.P. Raptopoulou, A. Terzis, E. Manessi-Zoupa, S.P. Perlepes, Mononuclear versus dinuclear complex formation in nickel (II) sulfate/phenyl (2-pyridyl) ketone oxime chemistry depending on the ligand to metal reaction ratio: Synthetic, spectral and structural studies, Spectrochim. Acta Mol. Biomol. Spect., 70 (2008) 718-728.
[21] I. Socorro, A. Neels, H. Stoeckli-Evans, AgI and CuI binuclear macrocyclic complexes with 1-(3-pyridyl) ethanone oxime, Acta Crystallogr. Sect. C: Cryst. Struct. Commun., 60 (2004) m13-m15.
[22] V.J. Argyle, L.M. Woods, M. Roxburgh, L.R. Hanton, Triflate anion and ligand influences in silver (I) coordination polymers of four isomeric dipyridyl ketone oximes, Cryst. Eng. Comm., 15 (2013) 120-134.
[23] C.J. Milios, T.C. Stamatatos, S.P. Perlepes, The coordination chemistry of pyridyl oximes, Polyhedron, 25 (2006) 134-194.
[24] K. Karami, Z.M. Lighvan, A.M. Alizadeh, M. Poshteh-Shirani, T. Khayamian, J. Lipkowski, Synthesis of a novel trinuclear palladium complex: the influence of an oxime chelate ligand on biological evaluation towards double-strand DNA, BSA protein and molecular modeling studies, RSC Adv., 6 (2016) 78424-78435.
[25] A. Pombeiro, V.Y. Kukushkin, J. McCleverty, T. Meyer, Comprehensive Coordination Chemistry II, vol. 1Elsevier, Amsterdam, 2004.
[26] P. Eyer, The role of oximes in the management of organophosphorus pesticide poisoning, Toxicolog. rev., 22 (2003) 165-190.
[27] R. Black, J. Harrison, The chemistry of organophosphorus chemical warfare agents, Patai's Chemistry of Functional Groups, (1996).
[28] J. Bajgar, Organophosphates/ Nerve Agent Poisoning: Mechanism of Action, Diagnosis, Prophylaxis, And Treatment, Adv. Clin. Chem., 38 (2004) 151-216.

[29] K. Kuca, D. Jun, K. Musilek, Structural requirements of acetylcholinesterase reactivators, Mini rev. med. chem., 6 (2006) 269-277.
[30] K. Musilek, M. Dolezal, F. Gunn□Moore, K. Kuca, Design, evaluation and structure—Activity relationship studies of the AChE reactivators against organophosphorus pesticides, Med. Res. Rev., 31 (2011) 548-575.
[31] E. Abele, R. Abele, E. Lukevics, Pyridine Oximes: Synthesis, Reactions, and Biological Activity, Chem. Heterocycl. Comp., 39 (2003) 825-865.
[32] C.F. Liu, C. Liu, An Investigation of the Complexes of Platinum (II) with Pyridine-2-aldoxime. cis-trans Isomerism1, J. Am. Chem. Soc., 83 (1961) 2615-2617.
[33] C. Liu, C.F. Liu, Complexes of Copper with Pyridine-2-aldoxime1, J. Am. Chem. Soc., 83 (1961) 4169-4172.
[34] C.F. Liu, C. Liu, Complexes between Palladium (II) and Pyridine-2-aldoxime, Inorg. Chem., 2 (1963) 706-707.
[35] R. Beckett, B. Hoskins, Crystal and molecular structure of a trinuclear copper (II) complex: μ 3-hydroxo-tri-μ-(pyridine-2-carbaldehyde oximato)-μ 3-sulphato-tricopper (II)–16· 3water, J. Chem. Soc., Dalton Trans., (1972) 291-295.
[36] E.S. Koumousi, M. Zampakou, C.P. Raptopoulou, V. Psycharis, C.M. Beavers, S.J. Teat, G. Psomas, T.C. Stamatatos, First palladium (ii) and platinum (ii) complexes from employment of 2, 6-diacetylpyridine dioxime: synthesis, structural and spectroscopic characterization, and biological evaluation, Inorg. chem., 51 (2012) 7699-7710.
[37] R. Clark, J. Reid, The analytical calculation of absorption in multifaceted crystals, Acta Crystallogr. Sect. A: Found. Crystallogr., 51 (1995) 887-897.
[38] J. Marmur, A procedure for the isolation of deoxyribonucleic acid from micro-organisms, J. Mol. Biol., 3 (1961) 208IN201-218.
[39] P. Sathyadevi, P. Krishnamoorthy, N.S. Bhuvanesh, P. Kalaiselvi, V.V. Padma, N. Dharmaraj, Organometallic ruthenium (II) complexes: Synthesis, structure and influence of substitution at azomethine carbon towards DNA/BSA binding, radical scavenging and cytotoxicity, Eur. J. Med. Chem., 55 (2012) 420-431.
[40] M. Reichmann, S. Rice, C. Thomas, P. Doty, A further examination of the molecular weight and size of desoxypentose nucleic acid, J. Am. Chem. Soc., 76 (1954) 3047-3053.
[41] V.A. Bloomfield, D.M. Crothers, I. Tinoco, Physical chemistry of nucleic acids, Harper & Row New York1974.
[42] R. Esteghamat-Panah, H. Hadadzadeh, H. Farrokhpour, J. Simpson, A. Abdolmaleki, F. Abyar, Synthesis, structure, DNA/protein binding, and cytotoxic activity of a rhodium (III) complex with 2, 6-bis (2-benzimidazolyl) pyridine, Eur. J. Med. Chem., 127 (2017) 958-971.
[43] N. Nanjundan, P. Selvakumar, R. Narayanasamy, R.A. Haque, K. Velmurugan, R. Nandhakumar, T. Silambarasan, R. Dhandapani, Synthesis, structure, DNA/BSA interaction and in vitro cytotoxic activity of nickel (II) complexes derived from S-allyldithiocarbazate, J. Photochem. Photobiol. B: Biol., 141 (2014) 176-185.
[44] E. Alarcon, A. Aspée, M. Gonzalez-Bejar, A. Edwards, E. Lissi, J. Scaiano, Photobehavior of merocyanine 540 bound to human serum albumin, Photochem. Photobiol. Sci., 9 (2010) 861-869.
[45] N.S. Quiming, R.B. Vergel, M.G. Nicolas, J.A. Villanueva, Interaction of bovine serum albumin and metallothionein, J. health sci., 51 (2005) 8-15.
[46] G.M. Morris, R. Huey, W. Lindstrom, M.F. Sanner, R.K. Belew, D.S. Goodsell, A.J. Olson, AutoDock4 and AutoDockTools4: Automated docking with selective receptor flexibility, J. Comput. Chem., 30 (2009) 2785-2791.
[47] G.M. Morris, D.S. Goodsell, R.S. Halliday, R. Huey, W.E. Hart, R.K. Belew, A.J. Olson, Automated docking using a Lamarckian genetic algorithm and an empirical binding free energy function, J. Comput. Chem., 19 (1998) 1639-1662.
[48] C. Hetényi, D. van der Spoel, Efficient docking of peptides to proteins without prior knowledge of the binding site, Protein Sci., 11 (2002) 1729-1737.
[49] C. Hetényi, D. van der Spoel, Blind docking of drug-sized compounds to proteins with up to a thousand residues, FEBS Lett., 580 (2006) 1447-1450.
[50] K. Karami, M. Alinaghi, Z. Amirghofran, J. Lipkowski, A.A. Momtazi-borojeni, A saccharinate-bridged palladacyclic dimer with a Pd–Pd bond: experimental and molecular docking studies of the

interaction with DNA and BSA and in vitro cytotoxicity against human cancer cell lines, New J. Chem., 42 (2018) 574-586.
[51] L. Pauling, The Nature of the Chemical Bond, Cornell university press Ithaca, NY1960.
[52] C.J. Milios, P. Kyritsis, C.P. Raptopoulou, A. Terzis, R. Vicente, A. Escuer, S.P. Perlepes, Di-2-pyridyl ketone oxime [(py) 2 CNOH] in manganese carboxylate chemistry: mononuclear, dinuclear and tetranuclear complexes, and partial transformation of (py) 2 CNOH to the gem-diolate (2−) derivative of di-2-pyridyl ketone leading to the formation of NO 3−, Dalton Trans., (2005) 501-511.
[53] R. Loganathan, S. Ramakrishnan, M. Ganeshpandian, N.S. Bhuvanesh, M. Palaniandavar, A. Riyasdeen, M.A. Akbarsha, Mixed ligand copper (II) dicarboxylate complexes: the role of co-ligand hydrophobicity in DNA binding, double-strand DNA cleavage, protein binding and cytotoxicity, Dalton Trans., 44 (2015) 10210-10227.
[54] K. Karami, M. Alinaghi, Z. Amirghofran, J. Lipkowski, Synthesis and characterization of two new trans palladium (II) complexes containing benzylamine ligand: DNA/BSA interactions, molecular docking and in vitro cytotoxic activity, Inorg. Chim. Acta, (2017).
[55] M.T. Carter, M. Rodriguez, A.J. Bard, Voltammetric studies of the interaction of metal chelates with DNA. 2. Tris-chelated complexes of cobalt (III) and iron (II) with 1, 10-phenanthroline and 2, 2'-bipyridine, J. Am. Chem. Soc., 111 (1989) 8901-8911.
[56] A. Dimitrakopoulou, C. Dendrinou-Samara, A.A. Pantazaki, M. Alexiou, E. Nordlander, D.P. Kessissoglou, Synthesis, structure and interactions with DNA of novel tetranuclear,[Mn 4 (II/II/II/IV)] mixed valence complexes, J. Inorg. Biochem., 102 (2008) 618-628.
[57] E.T. Wahyuni, D.H. Tjahjono, N. Yoshioka, H. Inoue, Spectroscopic studies on the thermodynamic and thermal denaturation of the ct-DNA binding of methylene blue, Spectrochim. Acta A: Mol. Biomol. Spect., 77 (2010) 528-534.
[58] R. Rohs, H. Sklenar, Methylene blue binding to DNA with alternating AT base sequence: minor groove binding is favored over intercalation, J. Biomol. Struct. Dyn., 21 (2004) 699-711.
[59] E.C. Long, J.K. Barton, On demonstrating DNA intercalation, Accounts of Chemical Research, 23 (1990) 271-273.
[60] Z.M. Lighvan, A. Abedi, M. Bordar, Novel mononuclear zinc complexes with 2, 2′-dimethyl-4, 4′-bithiazole: Synthesis, crystal structure and DNA-binding studies, Polyhedron, 42 (2012) 153-160.
[61] K. Karami, F. Parsianrad, M. Alinaghi, Z. Amirghofran, Cyclopalladated complexes containing metformin and benzylamine derivatives: Synthesis, characterization, binding interactions with DNA and BSA, in vitro cytotoxicity studies, Inorg. Chim. Acta, 467 (2017) 46-55.
[62] M. Anjomshoa, H. Hadadzadeh, S.J. Fatemi, M. Torkzadeh-Mahani, A mononuclear Ni (II) complex with 5, 6-diphenyl-3-(2-pyridyl)-1, 2, 4-triazine: DNA-and BSA-binding and anticancer activity against human breast carcinoma cells, Spectrochim. Acta A: Mol. Biomol. Spect., 136 (2015) 205-215.
[63] B.-d. Wang, Z.-Y. Yang, Q. Wang, T.-k. Cai, P. Crewdson, Synthesis, characterization, cytotoxic activities, and DNA-binding properties of the La (III) complex with Naringenin Schiff-base, Bioorg. Med. Chem., 14 (2006) 1880-1888.
[64] K. Karami, M. Alinaghi, Z. Amirghofran, J. Lipkowski, A saccharinate-bridged palladacyclic dimer with Pd-Pd bond: experimental and molecular docking studies of the interaction with DNA and BSA and in vitro cytotoxicity activities against human cancer cell lines, New J. Chem., 42 (2018) 574-586.
[65] R.A. Khan, F. Arjmand, S. Tabassum, M. Monari, F. Marchetti, C. Pettinari, Organometallic ruthenium (II) scorpionate as topo IIα inhibitor; in vitro binding studies with DNA, HPLC analysis and its anticancer activity, J. Organomet. Chem., 771 (2014) 47-58.
[66] R. Loganathan, S. Ramakrishnan, E. Suresh, A. Riyasdeen, M.A. Akbarsha, M. Palaniandavar, Mixed ligand copper (II) complexes of N, N-bis (benzimidazol-2-ylmethyl) amine (BBA) with diimine co-ligands: efficient chemical nuclease and protease activities and cytotoxicity, Inorg. Chem., 51 (2012) 5512-5532.
[67] M. Howe-Grant, K.C. Wu, W.R. Bauer, S.J. Lippard, Binding of platinum and palladium metallointercalation reagents and antitumor drugs to closed and open DNAs, Biochemistry (Mosc). 15 (1976) 4339-4346.
[68] E.R. Taylor, C.H. McGowan, Cleavage mechanism of human Mus81–Eme1 acting on Holliday-junction structures, Proc. Nat. Acad. Sci., 105 (2008) 3757-3762.

[69] H. Liu, Y.y. Kou, L. Feng, D.d. Li, C.Y. Gao, J.l. Tian, J.y. Zhang, S.p. Yan, Synthesis, structure and DNA cleavage of mononuclear Fe (III) complexes with 1, 2, 4□triazole□base ligand, Appl. Organomet. Chem., 24 (2010) 636-640.
[70] Q. Cheng, F. Zhang, H. Zhou, Z. Pan, G. Liao, DNA cleavage activities of two dinuclear copper coordination polymers, J. Coord. Chem., 68 (2015) 1997-2005.
[71] R. Vafazadeh, F. Jafari, M.M. Heidari, A.C. Willis, Alkyl chain length effect on construction of copper (II) complexes with tridentate Schiff base ligand and DNA interaction, J. Coord. Chem., 69 (2016) 1313-1325.
[72] X.-T. Zhang, Z.-Y. Ma, C. Zhao, Q.-J. Zhou, C.-Z. Xie, J.-Y. Xu, Synthesis, crystal structures, DNA binding, and cytotoxicity activities of two copper (II) complexes based on unsymmetrical tripodal ligands, J. Coord. Chem., 68 (2015) 2307-2323.
[73] M. Bhattacharyya, U. Chaudhuri, R. Poddar, Evidence for cooperative binding of chlorpromazine with hemoglobin: equilibrium dialysis, fluorescence quenching and oxygen release study, Biochem. Biophys. Res. Commun., 167 (1990) 1146-1153.
[74] H. Wang, X. Jiang, L. Zhou, Z. Cheng, W. Yin, M. Duan, P. Liu, X. Jiang, Interaction of NAEn-sn gemini surfactants with bovine serum albumin: a structure–activity probe, J. Lumin., 134 (2013) 138-147.
[75] J. Haribabu, K. Jeyalakshmi, Y. Arun, N.S. Bhuvanesh, P.T. Perumal, R. Karvembu, Synthesis, DNA/protein binding, molecular docking, DNA cleavage and in vitro anticancer activity of Nickel (II) bis (thiosemicarbazone) complexes, RSC Adv., 5 (2015) 46031-46049.
[76] A. Sułkowska, Interaction of drugs with bovine and human serum albumin, J. Mol. Struct., 614 (2002) 227-232.
[77] M. Van De Weert, Fluorescence quenching to study protein-ligand binding: common errors, J. fluores., 20 (2010) 625-629.
[78] J. Keizer, Nonlinear fluorescence quenching and the origin of positive curvature in Stern-Volmer plots, J. Am. Chem. Soc., 105 (1983) 1494-1498.
[79] Y.-J. Hu, Y. Liu, J.-B. Wang, X.-H. Xiao, S.-S. Qu, Study of the interaction between monoammonium glycyrrhizinate and bovine serum albumin, J. Pharm. Biomed. Anal., 36 (2004) 915-919.
[80] C.-H. Li, J.-H. Jiang, X. Li, L.-M. Tao, S.-X. Xiao, H.-W. Gu, H. Zhang, C. Jiang, J.-Q. Xie, M.-N. Peng, Synthesis, crystal structure and biological properties of a bismuth (III) Schiff-base complex, RSC Adv., 5 (2015) 94267-94275.
[81] R.L. Joseph, R. Lakowicz, Principles of fluorescence spectroscopy, Kluwer Academic/Plenum Publishers, New York, 1999.
[82] Y. Song, Y. Liu, W. Liu, F.A. Villamena, J.L. Zweier, Characterization of the binding of the Finland trityl radical with bovine serum albumin, RSC Adv., 4 (2014) 47649-47656.
[83] A. Mallick, B. Haldar, N. Chattopadhyay, Spectroscopic investigation on the interaction of ICT probe 3-acetyl-4-oxo-6, 7-dihydro-12H indolo-[2, 3-a] quinolizine with serum albumins, J. Phys. Chem. B, 109 (2005) 14683-14690.
[84] J.-Q. Tong, F.-F. Tian, Q. Li, L.-L. Li, C. Xiang, Y. Liu, J. Dai, F.-L. Jiang, Probing the adverse temperature dependence in the static fluorescence quenching of BSA induced by a novel anticancer hydrazone, Photochem. Photobiol. Sci., 11 (2012) 1868-1879.
[85] F. Deng, Y. Liu, Study of the interaction between tosufloxacin tosylate and bovine serum albumin by multi-spectroscopic methods, J. Lumin., 132 (2012) 443-448.
[86] Y. Yue, X. Chen, J. Qin, X. Yao, Characterization of the mangiferin–human serum albumin complex by spectroscopic and molecular modeling approaches, J. Pharm. Biomed. Anal., 49 (2009) 753-759.
[87] Y.-J. Hu, Y. Liu, L.-X. Zhang, R.-M. Zhao, S.-S. Qu, Studies of interaction between colchicine and bovine serum albumin by fluorescence quenching method, J. Mol. Struct., 750 (2005) 174-178.
[88] K. Karami, M. Hosseini-Kharat, H. Sadeghi-Aliabadi, J. Lipkowski, M. Mirian, In vitro cytotoxicity studies of palladacyclic complexes containing the symmetric diphosphine bridging ligand. Studies of their interactions with DNA and BSA, Eur. J. Med. Chem., 73 (2014) 8-17.
[89] E. Ulukaya, F. Ari, K. Dimas, E.I. Ikitimur, E. Guney, V.T. Yilmaz, Anti-cancer activity of a novel palladium (II) complex on human breast cancer cells in vitro and in vivo, Eur. J. Med. Chem., 46 (2011) 4957-4963.

[90] E. Ulukaya, F. Ari, K. Dimas, E.I. Ikitimur, E. Guney, V.T. Yilmaz, Anti-cancer activity of a novel palladium(II) complex on human breast cancer cells in vitro and in vivo, Eur. J. Med. Chem., 46 (2011) 4957-4963.
[91] C. Bincoletto, I.L. Tersariol, C.R. Oliveira, S. Dreher, D.M. Fausto, M.A. Soufen, F.D. Nascimento, A.C. Caires, Chiral cyclopalladated complexes derived from N, N-dimethyl-1-phenethylamine with bridging bis (diphenylphosphine) ferrocene ligand as inhibitors of the cathepsin B activity and as antitumoral agents, Bioorg. Med. Chem., 13 (2005) 3047-3055.
[92] A. Koch, P. Tamez, J. Pezzuto, D. Soejarto, Evaluation of plants used for antimalarial treatment by the Maasai of Kenya, J. Ethnopharmacol., 101 (2005) 95-99.
[93] M.P. Heng, S.K. Sinniah, W.Y. Teoh, K.S. Sim, S.W. Ng, Y.K. Cheah, K.W. Tan, Synthesis of a DNA-targeting nickel (II) complex with testosterone thiosemicarbazone which exhibits selective cytotoxicity towards human prostate cancer cells (LNCaP), Spectrochim. Acta A: Mol. Biomol. Spect., 150 (2015) 360-372.
[94] J.L. Hickey, R.A. Ruhayel, P.J. Barnard, M.V. Baker, S.J. Berners-Price, A. Filipovska, Mitochondria-targeted chemotherapeutics: the rational design of gold (I) N-heterocyclic carbene complexes that are selectively toxic to cancer cells and target protein selenols in preference to thiols, J. Am. Chem. Soc., 130 (2008) 12570-12571.
[95] M. Rakad, A. Jumaily, Evaluation of anticancer activities of crude extracts of Apium graveolens L. Seeds in two cell lines, RD and L20B in vitro, Iraq. J. Can. Med. Gen., 3 (2010) 20-23.
[96] A. abbas Momtazi-borojeni, M. Behbahani, H. Sadeghi-aliabadi, Antiproliferative activity and apoptosis induction of crude extract and fractions of avicennia marina, Iran. J. Bas. Med. Sci., 16 (2013) 1203.
[97] A.A. Momtazi, O. Askari-Khorasgani, E. Abdollahi, H. Sadeghi-Aliabadi, F. Mortazaeinezhad, A. Sahebkar, Phytochemical Analysis and Cytotoxicity Evaluation of Kelussia odoratissima Mozaff, J. Acupunct. Meridian Stud., (2017).
[98] R.M. Vaden, K.M. Gligorich, R. Jana, M.S. Sigman, B.E. Welm, The small molecule C-6 is selectively cytotoxic against breast cancer cells and its biological action is characterized by mitochondrial defects and endoplasmic reticulum stress, Breast Cancer Res., 16 (2014) 472.
[99] V. Zuco, R. Supino, S.C. Righetti, L. Cleris, E. Marchesi, C. Gambacorti-Passerini, F. Formelli, Selective cytotoxicity of betulinic acid on tumor cell lines, but not on normal cells, Cancer Lett., 175 (2002) 17-25.

Figure Captions:

Fig 1: ORTEP diagram for Pd(II) complex.

Fig 2: Electronic spectra of Pd(II) complex in buffer solution (5 mM Tris-HCl/10 mM NaCl at pH 7.2) upon addition of CT-DNA. [Complex] = (6×10^{-5}M), [DNA] = ($0\text{-}6\times10^{-4}$M). Arrow shows the absorption intensities decrease upon increasing DNA concentration. Inset: Plots of [DNA]/(ε_a-ε_f) vs. [DNA] for the titration of Pd(II) complex with CT-DNA.

Fig 3: Gel electrophoresis diagrams showing the cleavage of pUC57 DNA (0.01 M) at different concentrations of the Pd(II) complex and the oxime ligand in Tris–HCl/NaCl buffer (pH = 7.2) at 37°C for 3 h. Lane 1: marker;Lane 2: DNA control, Lane 3: DNA + Pd(II) complex (50 µM); Lane 4: DNA + Pd(II) complex (100 µM); Lane 5: DNA + Pd(II) complex (300 µM); Lane 6: DNA + Pd(II) complex (500 µM); Lane 7: DNA + Pd(II) complex (700 µM); Lane 8: DNA + Pd(II) complex (900 µM); Lane 9: DNA + oxime ligand (100 µM); Lane 10: DNA + oxime ligand (300 µM); and Lane 11: DNA + oxime ligand (500 µM).

Fig 4: Gel electrophoresis diagrams showing the cleavage of pUC57 DNA (0.01 M) by the Pd(II) complex and oxime ligand (700 µM) in Tris-HCl buffer (pH = 7.2) at 37ºC for 3 h in

the presence of DMSO, H_2O_2 and NaN_3 (700 μM). Lane 1: DNA control; Lane 2: DNA + Pd(II) complex + DMSO; Lane 3: DNA + Pd(II) complex + H_2O_2; Lane 4: DNA + Pd(II) complex + NaN_3; Lane 5: DNA + oxime ligand + H_2O_2; Lane 6: DNA + oxime ligand + H_2O_2 + DMSO; and Lane 7: DNA + oxime ligand + H_2O_2 + NaN_3.

Fig 5: UV absorption spectra of [BSA] = (6×10^{-6}M) in the absence and presence of different concentration of Pd(II) complex (0-6×10^{-5}M).

Fig 6: Emission spectra of BSA upon the titration of Pd(II) complex. [BSA] = (6×10^{-6}M), [complex] = (0-6×10^{-5}). Arrow shows the change upon the increasing complex concentration. Inset: Plots of I_0/I vs [Q]$\times10^6$.

Fig 7: Spectral overlaps of the absorption spectra of Pd(II) complex with the fluorescence spectra of BSA.

Fig 8: (A) Results of docking procedure of Pd(II) complex with the minor groove binding to the DNA, (B) The bases of DNA interactions with Pd(II) complex in the active site.

Fig 9: (A) Results of docking procedure of Pd(II) complex in the interaction with BSA residues, which results in quenching, (B) The BSA amino acid residues in interaction with Pd(II) complex.

Table 1: Crystallographic data and structure refinement details for Pd(II) complex.

Pd(II) complex	
Empirical formula	$C_{12}H_{14}N_4O_4P_0Pd$
Formula weight	384.67
T/K	150 (1)
Crystal system	Triclinic
Space group	P1
a/Å	7.4056 (6)
b/Å	8.9741 (8)
c/Å	10.6709 (9)
α/°	109.898 (3)
β/°	96.053 (4)
γ/°	90.052 (4)
v/ Å^3	662.60 (10)
Crystal dimensions / mm^3	0.12 × 0.11 × 0.08
Z	2
μ(mm^{-1})	11.53
D_{calc}/ Mg m^{-3}	1.928
F_{000}	384
Θ range/°	4.4–54.4
Independent reflections	1609
Data/restraints/parameters	12650/61/192
Goodness-of-fit on F^2	1.118
Final R indices	R_1= 0.0518, wR_2= 0.1384
R indices (all data)	R_1= 0.0576,wR_2= 0.1455
Largest difference peak and hole / e Å^{-3}	1.69, −0.92
CCDC number	1827296

Table 2: Selected bond lengths (Å), and angles (°) for Pd(II) complex.

Bond lengths		Bond angels	
Pd1-N1	2.031 (9)	N1—Pd1—N2	80.2 (4)
Pd1-N2	2.035 (8)	N3—Pd1—N2	99.9 (3)
Pd1-N3	2.041 (9)	N4—Pd1—N2	179.5 (3)
Pd1-N4	2.035 (8)	N3—Pd1—N1	178.9 (3)
O1-N1	1.283 (11)	N4—Pd1—N1	100.3 (4)
O2-N3	1.272 (11)	N4—Pd1—N3	79.7 (3)

Table 3: Estimated binding constants for site marker competitive experiments of the complex-BSA system.

System	K_b (M^{-1})	n	R
Complex-BSA	3.71×10^4	1.025	0.9974
Complex-BSA-Warfarin	2.50×10^4	0.91	0.9910
Complex-BSA-Ibuprofen	3.59×10^4	1.08	0.9914
Complex-BSA-Digoxin	3.58×10^4	0.99	0.9961

Table 4: Selective cytotoxicity data IC_{50} (µM) of the compounds against cancer and normal cell lines.

Compound	IC_{50} (µM) ± SD		
	C26	B16-F0	NIH
Oxime ligand	4.2±1	2.9 ± 4	>100
Pd(II) complex	2.7±2	2.0±1	>100
Cis-platin	17.0± 1	26.0 ± 1	38.67± 4

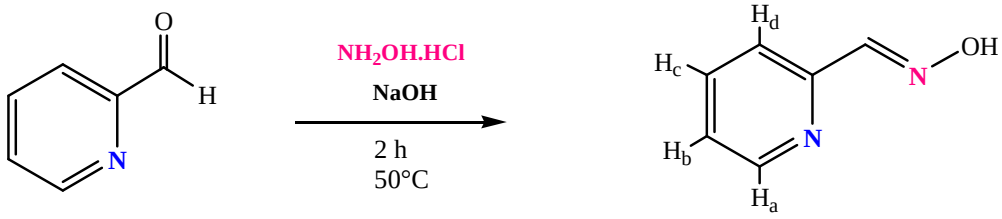

2-pyridine carboxaldehyde

pyridine-2-carbaldehyde oxime ligand

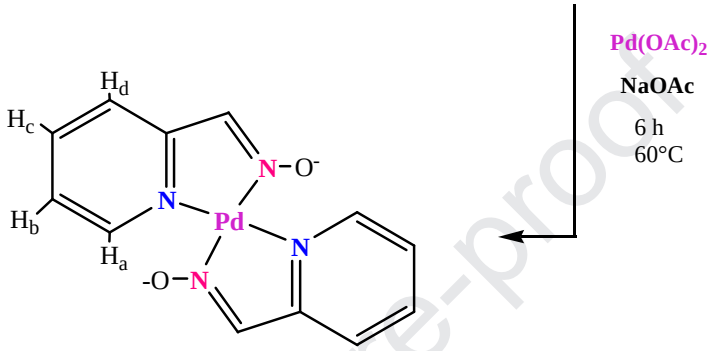

Pd(II) complex

Scheme 1: Synthetic route for the preparation of pyridine-2-carbaldehyde oxime ligand and Pd(II) complex.

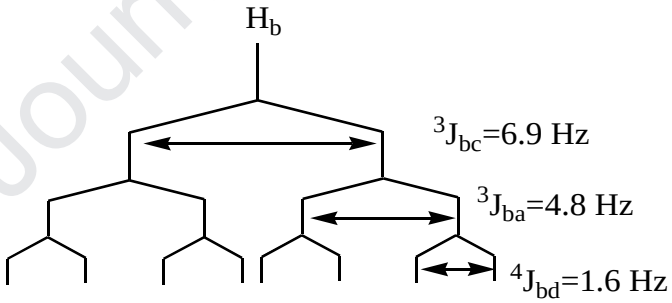

Scheme 2: splitting pattern of H_b in ^{1}HNMR spectra of oxime ligand.

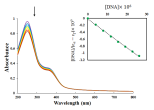

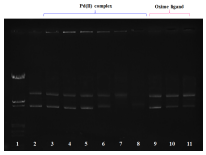

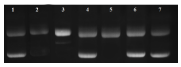

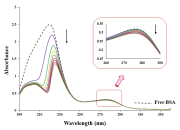

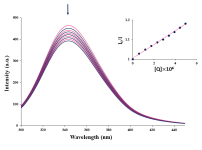

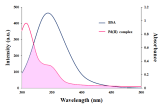

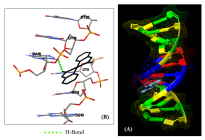

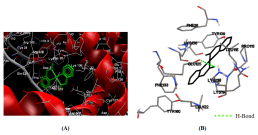

(A)

(B)

Highlights

- A new Pd(II) complex bearing pyridine-2-carbaldehyde oxime ligand has been synthesized and characterized.
- The interaction of Pd(II) complex with CT-DNA occurs by groove binding.
- The Pd(II) complex cleaves the supercoiled double-stranded DNA.
- The reactivity towards BSA showed a static emission quenching by the complex.
- *In vitro* cytotoxicity for Pd(II) complex, ligand and cisplatin were carried out against cancer and normal cell lines.

Declaration of interests

☒ The authors declare that they have no known competing financial interests or personal relationships that could have appeared to influence the work reported in this paper.

☐The authors declare the following financial interests/personal relationships which may be considered as potential competing interests: